Percolation transition in the porous structure of latex-templated silica monoliths

François Guillemot, Aline Brunet-Bruneau, Elodie Bourgeat-Lami, Jean-Pierre Boilot, Etienne Barthel, Thierry Gacoin

Percolation transition in the porous structure of latex-templated silica monoliths

François Guillemot[†,§], Aline Brunet-Bruneau[°], Elodie Bourgeat-Lami[◊], Jean-Pierre Boilot[†,], Etienne Barthel[§], Thierry Gacoin[†]*

[†]Groupe de Chimie du Solide, Laboratoire de Physique de la Matière Condensée, UMR CNRS 7643, Ecole Polytechnique, 91128 Palaiseau, France,

[§]Surface du Verre et Interfaces (CNRS/Saint-Gobain) UMR CNRS 125, 39 quai Lucien Lefranc, F-93303, Aubervilliers, France,

[°]Institut des Nanosciences de Paris, UMR CNRS 7601, Université Paris 6, Campus Boucicaut, 140 rue de Lourmel, case 80, 75015 Paris, France,

[◊]Laboratoire de Chimie, Catalyse, Polymères et Procédés (C2P2), UMR CNRS 5265 Université Lyon 1, CPE Lyon, CNRS, Bâtiment 308 F, 43 boulevard du 11 novembre 1918, BP 2077, 69616 Villeurbanne Cedex, France

Corresponding author. Jean-Pierre Boilot, Tel. (33)-1- 69 33 46 51. Fax : (33)-1- 69 33 47 99. Email: jean-pierre.boilot@polytechnique.edu.

Abstract

Porous sol-gel silica monoliths are prepared using PMMA nanoparticles, 60 nm in diameter, as sacrificial templates. The pore-structure of the calcined pellets is investigated through nitrogen adsorption to assess the evolution of the porosity when varying the amount of porogen. The latex templated monoliths present a well defined spherical extrinsic porosity and an intrinsic microporosity due to preparation process. As a result of a careful analysis of the adsorption hysteresis, we identify a percolation threshold of the spherical porosity around 30% volume fraction. This phenomenon, similar

to the percolation previously observed in latex-templated silica films, opens the way to the use of latex-templated porous silica monoliths with a tailorable and reliable pore structure.

Keywords: mesoporous silica monoliths – Latex templated silica – sol-gel silica- Porosity percolation – adsorption isotherms

Highlights

Porous silica sol-gel monoliths are prepared using PMMA nanoparticles as sacrificial templates.

Materials present a well defined pore structure with a straightforward pore volume adjustment.

We identify a percolation threshold of the spherical porosity around 30% volume fraction.

The porous structure is close to the one of analog films opening the way to combined characterizations.

1. Introduction

Porous silica monoliths of centimeter size with a well-defined pore structure are of high interest for applications taking advantage of either the high pore volume (filtration [1,2], fundamental physics experiments [3,4], template effect [5-7], insulation [8]) or the specific surface area : sensing [9] or catalysis [10].

The usual practice consists in preparing such monoliths from evaporation-induced self assembly (EISA) of amphiphilic molecules (surfactant and block polymers) [11,12] resulting in a variety of geometries and pore sizes under 30-40 nm. However, the porosity is sometimes inhomogeneous and the parameters of the porosity (pore size, pore volume fraction, pore structure geometry) cannot be adjusted independently. For many of the applications mentioned above, it is desirable to produce materials with monodisperse porosity and with easily tunable volume fraction (or surface specific area). This cannot be obtained with surfactant templating as the parameters of the porosity (pore size, pore organization, connectivity and pore volume fraction) are tightly correlated. Some porous materials with more easily adjustable pore volume fraction can be prepared by dispersing a demixing organic phase, however this is at the expense of the control on the pore shape, as the resulting porosity is often worm-like. Some work in the literature report the use of preformed organic nanoparticle (polymeric beads) sedimented in the form of a colloidal crystal and then infiltrated by a sol-gel sol to prepare the corresponding hollow crystal [13,14]. In this case, the pore volume fraction is restricted to the packing density of the initial colloidal crystal.

We have shown recently the interest of using polymer beads as a template for the preparation of porous silica thin films for optical applications. One of the strength of the technique is that the parameters of the porosity can be adjusted independently [15]. The specificity of such porous materials is that their pore structure (surface specific area) is easily described with simple geometrical considerations and we have thus demonstrated the existence of a well-defined pore percolation threshold. However, the preparation of the sol-gel bulk samples differs from the one of thin films resulting in most of cases in structural discrepancies [16].

This paper aims at demonstrating the interest of a similar approach to prepare porous silica monoliths. We shall illustrate the versatility of the approach using latex as template based on a comparison of pore structures in monolith and in thin films.

2. Experimental methods

2.1. Materials.

Tetraethylorthosilicate (TEOS, 98%), methylmethacrylate (MMA, 99%), ammonium persulfate (APS, 98%) were purchased from Aldrich. The anionic surfactant Disponil® FES 32 IS was graciously provided by Cognis as a solution of 32 wt% active matter in water. Absolute ethanol (99%) was purchased from Carlo Erba.

2.2. Porogen.

PMMA latex nanoparticles dispersion (A) were prepared by conventional emulsion polymerization of MMA initiated by APS in water, at 70°C, in a thermostated reactor under mechanical stirring. Disponil® FES 32 IS was used as surfactant.

2.3. Porous silica monoliths.

The silica sol (B) was prepared by mixing 14.2 mL of TEOS ($6.4\ 10^{-2}$ mol), 11.2 mL of ethanol and 4.62 mL of an HCl solution in deionised water with a pH=2.5. The sol was hydrolyzed at 60°C under reflux for 1 hour corresponding to the complete TEOS hydrolysis, as checked by ^{29}Si NMR spectroscopy. Then 20 mL of the HCl solution was added to the mixture and the ethanol was removed under vacuum. Ethanol was evaporated from the hydrolysed sol as it might destabilize the latex suspension. The volume of the final solution was adjusted to 22 mL with a pH=2.5 HCl solution to fix the silicon concentration to 2.90 mol.L^{-1}. The residual amount of ethanol was determined to be less than 5 vol.% by ^{1}H NMR spectroscopy.

The final sols were prepared by mixing A and B in various relative amounts to adjust the porous fraction and kept in closed cylindrical polypropylene vessels. Gelation occurred after a few days and the

vessels were slightly opened to let water evaporate slowly. After 15 days, the size of the monoliths was stabilized, and they could undergo pyrolysis of the organic template during 48 hours at 450°C.

2.4. Materials characterization

Scanning electron microscopy (SEM) with a field-effect gun (ZEIS Gemini DSM 982) was operated at voltages between 10 and 20 kV. Samples were mounted on to carbon coated SEM stubs and sputter coated with 2-3 nm of Platinum.

The surface area and pore sizes of the synthesized materials were determined by nitrogen physical adsorption using a Micromeritics ASAP 2001 porosimeter. A preliminary degassing of the samples was performed during 24 hours by heating at 150 °C under vacuum. The surface area was calculated using the Brunauer-Emmett-Teller (BET) method. Pore size distributions were calculated using the Barrett-Joyner-Halenda (BJH) method from the adsorption and desorption branches.

Nanoindentation tests were investigated by using an instrumented nanoindenter XP (MTS) with a Berkovich tip. 3 μm deep indents were performed in the porous monoliths and the harmonic modulus and hardness were measured on the plateau of the indentation curves.

3. Results and Discussion

Gelation of silica monoliths was obtained under ambient conditions with composite sol containing custom-made latex and tetraethylorthosilicate (TEOS), as previously described [15]. Drying was carried out within 15 days and the polymer phase was removed by pyrolysis. The porous fraction was tailored by varying the parameter P defined as follows:

$$P = \frac{V_{PMMA}}{V_{SiO_2} + V_{PMMA}}$$

Where V_{SiO_2} and V_{PMMA} are the corresponding volumes of the silica (related to the silicon concentration) and PMMA phases determined from their mass taking their respective densities equal to 2.20 (fused silica) and 1.18. This parameter corresponds to the volume fraction of polymer beads in the final silicate composite, further abbreviated as the latex volume fraction.

From the fracture surface of the monoliths we can observe that the pores are spherical and well dispersed in the whole silica matrix (Fig. 1). The increasing number of visible pores is in good agreement with the increase of the latex volume fraction in the initial sol.

The pore structure of the latex templated silica monoliths was then analysed carefully through nitrogen adsorption experiments for various latex volume fractions. Nitrogen sorption isotherms (Fig. 2a and 2b) are of common IV type [17] with a H1-type hysteresis observed in the range of relative partial pressure above 0.40. The evolution of the BET specific surface area S_{BET} determined on the first part of the adsorption isotherm can be expected to follow a simple geometrical evolution (see Supplementary data for details):

$$S_{BET} = \frac{6}{D_{latex} d_{SiO2}} \frac{P}{1-P} + S_{\mu} \qquad \text{(Eq.1)}$$

Where D_{latex} is the diameter of the latex template beads and d_{SiO2} the density of silica (2.2 g.cm^{-3}). The offset S_{μ} is the part of the surface specific area that is due to intrinsic microporosity in the silica walls. We have previously shown [15] that one of the most remarkable point in latex templated silica films prepared with the same method is that negligible amount of microporosity seems to be trapped in the silica matrix. If compared with thin films, this is not the case in porous silica monoliths where an intrinsic microporosity is usually present due to a lower effect of the capillary stresses during the drying process. Values reported in the literature for this S_{μ} are in the 500-550 m^2.g^{-1} for silica cured at 450°C [16].

The evolution of the BET surface specific area as a function of the latex volume fraction P is presented in Fig. 3. The dotted line represents the evolution expected based on Eq. 1 with a latex diameter D_{latex} of 50 nm and a microporous surface specific area S_{μ} of 500 m^2.g^{-1}. The diameter of the latex beads in suspension in water was measured initially to be 60 nm (dynamic light scattering, DLS). The small discrepancy between the original diameter of the beads and the diameter extrapolate from the

BET surface specific area evolution can be the result of the shrinkage of the monoliths after the latex was removed by pyrolysis (silica network condensation). This corresponds to the estimated 20% shrinkage than can be checked on SEM pictures (Fig. 1) measuring the pore size in comparison to the DLS particle size.

These question about pore size can be more precisely resolved by a BJH analysis of both the adsorption and the desorption branches of the nitrogen sorption isotherms [18]. The analysis of the adsorption branch reveals a pore size around 50 nm corresponding to the capillary condensation observed above a relative partial pressure of 0.9 (Fig. 4a). The model behaviour of these latex templated monoliths is confirmed by the observation of well-defined pores (about 50 nm in size), with a similar distribution of the starting latex, and a continuum growing for small pore sizes (under 4 nm) corresponding to the microporosity. Note that for the P=70% sample, some shrinking of the structure seems to occur.

The most specific information about the particular structure of the porosity is given by analysing the desorption branch of the hysteresis. As can be seen in Fig. 2a and 2b the hysteresis shape on the adsorptions isotherms changes while the latex volume fraction is increasing. For low latex volume fraction, the hysteresis is wide and almost of a rectangular shape (with desorption around P/P_0 =0.45). As the latex volume fraction increases, the desorption branch begins to move towards higher relative partial pressure (begins for P=30%) and reaches P/P_0=0.85 for P=60%. The BJH pore size distribution (PSD) obtained by the analysis of the desorption branch reflects these observations (Fig. 4b), with a strong peak around 4 nm observed for low latex volume fraction. Increasing latex volume fraction, this peak decreases simultaneously with the growth of a wide population in the 10-20 nm range.

This phenomenon can be interpreted as the progressive opening of throats between extrinsic spherical pores created with latex beads [17,19]. During desorption, the drain occurs at the relative partial pressure given by Kelvin's equation considering the size characteristic of the porosity regarding desorption. In a ink-bottle shape model, the characteristic size for desorption is the size of the neck of the bottle, whereas

for adsorption it is the bigger dimension in the bottle. In the case of latex templated silica monoliths, the size of interest for the desorption may vary depending on the latex volume fraction P (Fig. 5). For low values of P, the spherical pores will not be in contact with each other, so that the characteristic size for nitrogen desorption will be the size of the micropores that make the link between the spherical pore and the atmosphere. As the latex volume fraction P is growing, some contact between spherical pores may occur, and some of these pores may communicate. We can interpret the changes in the desorption PSD in the field of an opening of such communications between spherical pores.

This result may be compared to what the author previously observed for latex templated silica films [15]. In this case, the pore structure is more simple with a negligible microporosity in the films and a percolation transition for the porosity has been shown with a threshold value of P=40-45%. At this threshold, all the porosity becomes suddenly connected with contacts between the spherical pores. For porous silica monoliths, such a threshold should modify the sorption isotherm by changing the position of the desorption branch due to the opening of the communication between the spherical pores. This is what is observed experimentally, so that we may interpret the change of the hysteresis shape as a piece of evidence of the percolation of the spherical porosity in the silica monoliths. Above the threshold, the 'bottle-neck' shaped passage between pores opens progressively leading to some functional way in the porous silica monoliths.

The mechanical properties of the porous silica monoliths were measured by nanoindentation and are presented in Table 1. As expected for porous materials, the elastic modulus decreases as the pore volumes fraction increases. . The values measured on the latex-templated silica monoliths are slightly lower (7 GPa for a latex volume fraction of 0.5) than the ones measured on porous silica films (11 GPa for a film with the same latex volume fraction). This probably arises from the slightly higher porous fraction in the monoliths due to the higher fraction of microporosity. As for the thin film system, no drastic change in the mechanical properties is observed at the percolation threshold.

Such a strong similarity between the structure of a sol-gel silica film and a sol-gel silica monolith is quite rare and represents an interesting academic tool. Indeed, many experimental characterizations are

inapplicable on thin films for sensitivity reasons (not enough material) or because of strong parasitic effect (e.g. susbtrate effects for mechanical characterizations). This work opens the way to a combined characterization of the properties of porous silica films with the help of more macroscopic characterization on latex-templated silica monoliths.

4. Conclusion

On the field of preparation of porous silica monoliths, we have been able to prepare porous materials with a well defined pore structure consisting in spherical pores with a well defined diameter linked together by a worm-like microporous network. This synthesis approach leads to porous monoliths with a reproducible pore structure while changing the pore volume fraction. A porosity percolation transition with the opening of the spherical pore interconnection was thus observed at a pore fraction threshold of about 30% volume fraction as previously observed in latex-templated silica films.

Acknowledgements

FG deeply acknowledges Saint-Gobain for financial support and A. Lelarge for SEM pictures. The authors thank J. Teisseire and N. Chemin for fruitful discussions.

References

[1] K. Nakanishi and N. Tanaka, Acc. Chem. Res. 40(9) (2007) 863–873.

[2] S. Hartmann, D. Brandhuber, and N. Hüsing, Acc. Chem. Res. 40(9) (2007) 885–894.

[3] P. Perez and A. Rosowsky, Nuclear Instruments and Methods in Physics Research A. 545(1-2) (2005) 20–30.

[4] L. Liszkay, C. Corbel, L. Raboin, J.-P. Boilot, P. Perez, A. Brunet-Bruneau, P. Crivelli, U. Gendotti, A. Rubbia, T. Ohdaira, and R. Suzuki, Appl. Phys. Lett. 95(12) (2009) 124103.

[5] Z. Wang, F. Li, N. S. Ergang, and A. Stein, Chem. Mater. 18(23) (2006) 5543–5553.

[6] F. Schüth, Chem. Mater. 13(10) (2001) 3184–3195.

[7] C. M. Doherty, R. a. Caruso, B. M. Smarsly, and C. J. Drummond, Chem. Mater. 21 (13) (2009) 2895–2903.

[8] G. M. Pajonk, Colloid Polym. Sci. 281(7) (2003) 637–651.

[9] S. A. El-Safty, D. Prabhakaran, A. A. Ismail, H. Matsunaga, and F. Mizukami, Chem. Mater. 20(8) (2008) 2644–2654.

[10] M. G. Bellino, A. E. Regazzoni, and G. J. a. a. Soler-Illia, ACS Appl. Mater. Interfaces. 2(2) (2010) 360–365.

[11] S. A. El-Safty, J. Porous Mater. 15(4) (2007) 369–387.

[12] Y. Wan and D. Zhao, Chem. Rev. 107(7) (2007) 2821–2860.

[13] B. T. Holland, C. F. Blanford, T. Do, and A. Stein, Chem. Mater. 11(3) (1999) 795–805.

[14] P. Yang, T. Deng, D. Zhao, P. Feng, D. Pine, B. F. Chmelka, G. M. Whitesides, and G. D. Stucky, Science. 282(5397) (1998) 2244–2246.

[15] F. Guillemot, A. Brunet-Bruneau, E. Bourgeat-Lami, T. Gacoin, E. Barthel, and J.-P. Boilot, Chem. Mater. 22(9) (2010) 2822–2828.

[16] C. J. Brinker and G. W. Scherer, Sol-Gel Science: The Physics and Chemistry of Sol-Gel Processing, Academic Press, (1990) 717.

[17] K. S. W. Sing, D. H. Everett, R. Haul, L. Moscou, R. Pierotti, J. Rouquerol, and T. Siemieniewska, Pure Appl. Chem. 57(4) (1985) 603 – 619.

[18] E. P. Barrett, L. G. Joyner, and P. P. Halenda, J. Am. Chem. Soc. 73(1) (1951) 373–380.

[19] J. W. Mcbain, J. Am. Chem. Soc. 57(4) (1935) 699–700.

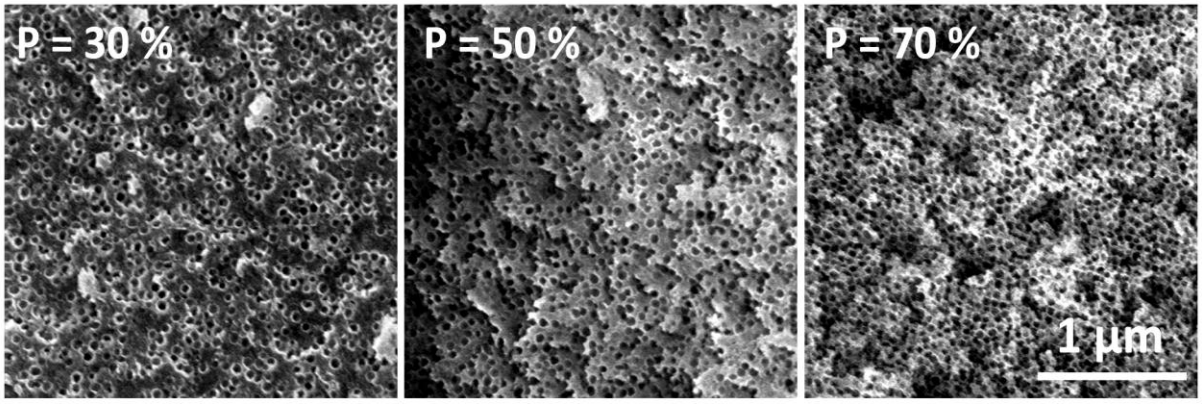

Fig. 1. SEM pictures of porous monoliths prepared with an increasing amount of latex beads (60 nm) regarding silica.

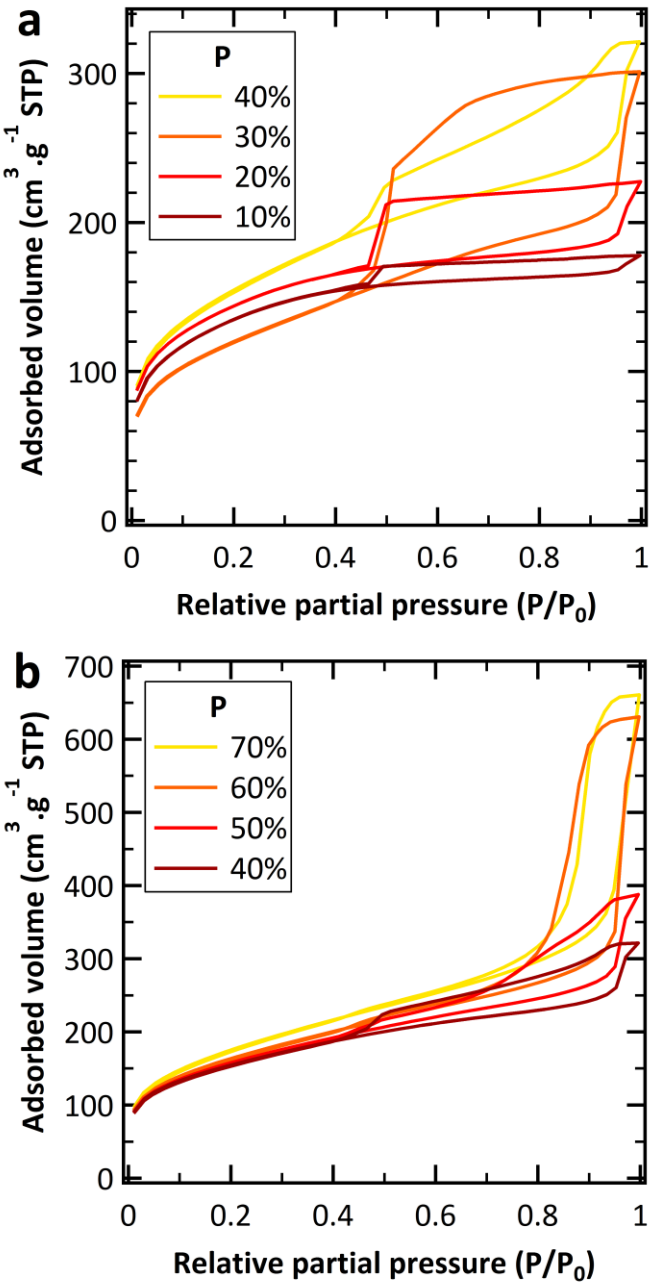

Fig. 2. BET N_2 adsorption isotherms in porous silica monoliths templated by a 60 nm latex with various latex volume fraction P. (a) P ranging from 10% to 40%. (b) P ranging from 40% to 70%.

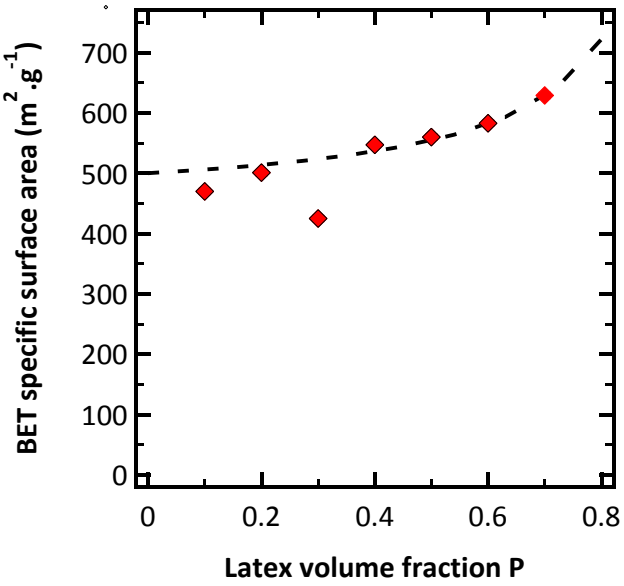

Fig. 3. Evolution of the BET specific surface area for silica monoliths templated by a 60 nm latex with the latex volume fraction. The dotted line represents the evolution expected with the geometrical model (equation 1) taking S_μ at 500 $m^2.g^{-1}$ and D_{latex} at 50 nm.

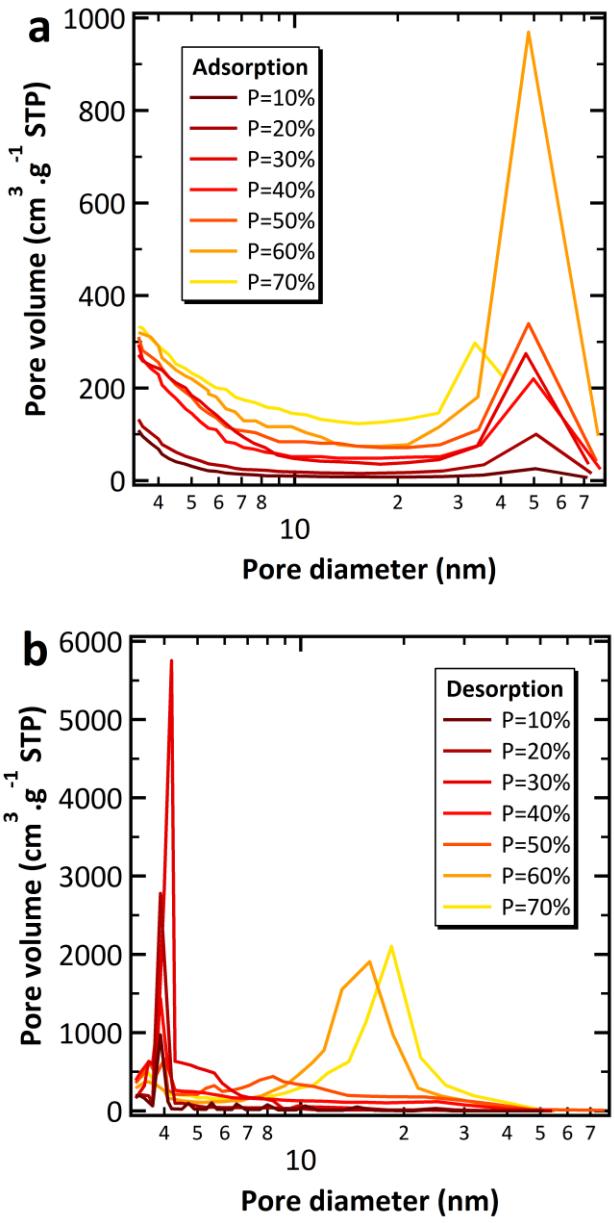

Fig. 4. BJH pore size distribution (PSD) in silica monoliths templated with a 60 nm latex determined on the adsorption branch (a) or the desorption branch (b) of the nitrogen adsorption isotherms for various latex volume fraction P.

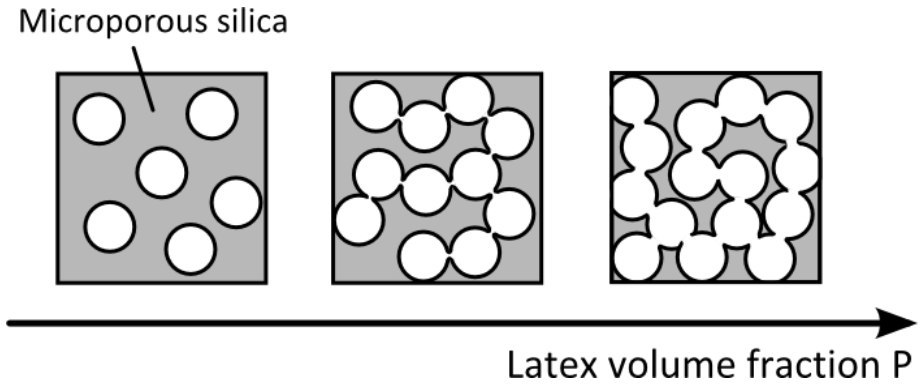

Fig. 5. Schematic representation of the opening of necks between the spherical pores.

Table 1: Harmonic modulus measured by nanoindentation on porous silica monoliths prepared with latex volume fraction from 0.3 to 0.7.

Latex Volume Fraction	**Harmonic Modulus (GPa)**
0.3	16 +/- 1
0.4	10 +/- 1
0.5	7 +/- 1
0.6	5 +/- 1
0.7	2 +/- 1

Supplementary data

1. NMR characterization.

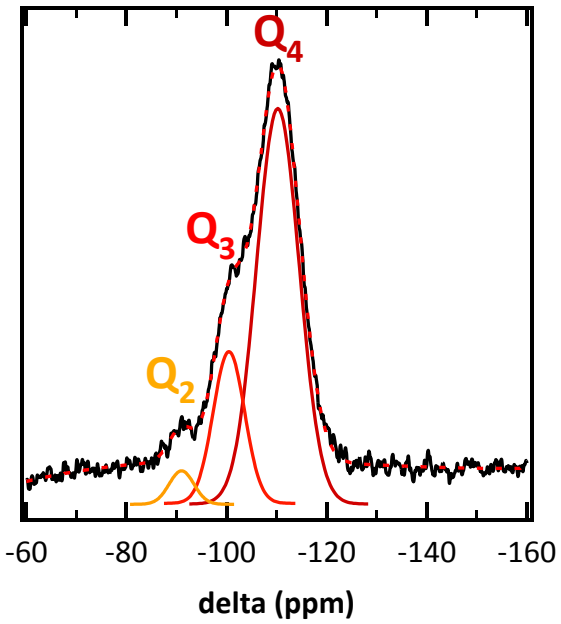

	Q_2	Q_3	Q_4
δ (ppm)	-90	-100	-110
Area (%)	3.7	21.2	75.1

Fig. S1. NMR ^{29}Si of porous silica monolith after curing at 450°C. Spectral deconvolution between common Q_2, Q_3 and Q_4 tetrahedral units is overlaid on the spectrum, and summed-up in the table on the right. (TecMag Apollo 360 Spectrometer, 71.54 MHz, 7 mm DOTY probe, 45° pulse, rotation 4.9 kHz).

2. Geometrical considerations on the specific surface area in latex templated monoliths.

If all the BET surface-area S_{BET} is coming from the latex templated pores, one should expect:

$$S_{BET} = \frac{S_{PMMA}}{m_{tot}} + S_{\mu} \quad (1)$$

With S_{PMMA} the surface of the initial latex beads embedded in the monolith, m_{tot} the total mass of the monolith and S_{μ} the contribution of the microporosity to the specific surface area.

S_{PMMA} can be linked to the latex volume fraction P as :

$$P = \frac{V_{PMMA}}{V_{tot}} \quad (2)$$

With V_{PMMA} the volume of the initial latex beads embedded in the monolith, and V_{tot} the total volume of the monolith.

This leads to:

$$S_{PMMA} = \frac{6}{D_{latex}} PV_{tot} \quad (3)$$

With D_{latex} the diameter of the spherical beads composing the latex.

On the other hand, m_{tot} in equation (1) can be replaced by:

$$m_{tot} = V_{tot} d_{tot}$$

$$m_{tot} = V_{tot} (1 - P) d_{SiO_2} \quad (4)$$

With d_{tot} and d_{SiO_2} the respective densities of the monolith and vitreous silica.

Gathering equations (3) and (4) in equation (2) leads to :

$$S_{BET} = \frac{6}{D_{latex} d_{SiO2}} \frac{P}{1 - P} + S_{\mu}$$